RSC Advances

PAPER

View Article Online
View Journal | View Issue

Cite this: *RSC Adv.*, 2025, **15**, 9420

Novel fabrication of biodegradable superabsorbent polymer from wheat stalk for water holding and sustained fertilizer release

Yang Chenxi, *[abcde] Wang Jian,[abcd] Wang Yingguo,[abcd] Zhang Haiou[abcd] and He Puchun[abcd]

Water-retaining agents have been shown to significantly improve the efficiency of irrigation water use in long-term agricultural activities, outperforming traditional irrigation methods. However, existing water-retaining agents still face challenges related to cost-effectiveness and degradability. To address these issues, we developed a superabsorbent material composed of wheat stalk (WS) and polyacrylic acid (PAA)–polyacrylamide (PAM), fabricated *via* versatile polymerization techniques. The integrated properties of the material, including water absorbency, water holding capacity, urea sustained-release behavior, and soil degradation, were thoroughly evaluated. The results indicated that WS/PAA–PAM exhibited a water absorption capacity of 273.54 g g^{-1} in deionized water and 44.54 g g^{-1} in saline solution, demonstrating excellent water retention properties. Kinetic studies revealed that water diffusion followed Fick diffusion, and the swelling process could be described by a first-order kinetic model. Notably, the material maintained high water absorption even after three cycles of re-swelling. Furthermore, WS/PAA–PAM effectively controlled the release of urea, minimizing fertilizer loss due to runoff, thereby promoting sustained nutrient delivery. These findings highlight the potential of WS/PAA–PAM as a cost-effective, biodegradable water and fertilizer management solution, offering a promising strategy for improving water and fertilizer utilization efficiency in future agricultural applications.

Received 7th January 2025
Accepted 17th February 2025

DOI: 10.1039/d5ra00143a

rsc.li/rsc-advances

1 Introduction

Agriculture plays a significant role in human development, particularly in low-income and developing countries.[1] However, scarcity of water resources poses a serious challenge to agriculture and food production. To address this issue, technological strategies include the construction of reservoirs and canal infrastructure to enhance water supply security, as well as the implementation of advanced irrigation techniques to improve irrigation water use efficiency.[2] Among various methods, water-retaining superabsorbents are one of the most promising strategies for alleviating water shortages in agriculture, as they can absorb water and reduce ineffective evaporation.[3,4] Generally, water-holding agents are hydrophilic materials. The action mechanism is that the hydrophilic materials absorb liquid water through the network structure of hydrophilic groups, then sustained release this absorbed water to the soil. Moreover, adding water holding superabsorbent to arid soil could improve the looseness and porosity of soil, water holding capacity and accelerate the seed germination and root growth.[5] In recent years, water-holding agents have included synthetic (polyacrylic (PAA), polyacrylamide (PAM) and polyacrylonitrile),[6,7] semi-synthetic (halloysite),[8] and natural materials derived from raw sources (cellulose *et al.*).[9] For instance, Liu *et al.*[5] synthesized borax-crosslinked fenugreek galactomannan hydrogel through a one-step method, enhancing its thermal stability. When combined with sandy soil, the hydrogel powder improved the soil's water absorption and retention capacity. Song *et al.*[10] prepared a HA water-retaining agent (HAA) *via* aqueous polymerization of potassium humate, sodium carboxymethyl cellulose, acrylic acid, and bentonite. Pea seedling growth tests showed that the germination rate in the HAA-PU group exceeded 60%, compared to the soil control group. However, despite the proven effectiveness of synthetic water-retaining agents, their practical application in farmland water conservation remains limited. The high cost of both the substrates and the preparation processes significantly hampers their widespread use. Additionally, some synthetic substrates used in these agents may introduce harmful substances into the soil, potentially compromising soil health and crop safety. These challenges underscore the need for cost-effective, environmentally

[a]*Institute of Land Engineering and Technology, Shaanxi Provincial Land Engineering Construction Group Co., Ltd, China. E-mail: 1098002212@qq.com*
[b]*Shaanxi Agricultural Development Group Co., Ltd, China*
[c]*Key Laboratory of Degraded and Unused Land Consolidation Engineering, Ministry of Natural Resources, China*
[d]*Shaanxi Engineering Research Center of Land Consolidation, China*
[e]*Land Engineering Technology Innovation Center, Ministry of Natural Resources, China*

friendly alternatives that can achieve both effective water retention and minimal ecological impact.[11] Herein, a novel water-retaining agent using cheap substrate with excellent biodegradability provide a promising perspective for designing advanced water retaining agents.

In agricultural production, sustainable agriculture play crucial roles in promoting the betterment of soil, water, air, and the overall ecology and environment.[12] In consequence, sustainable agriculture activities could be crucial ways to accelerate sustainable development and improve resource utilization.[13] To maintain the continuous growth of crop yield and alleviate food security, the rational utilization of agricultural waste is innovative agricultural strategies.[12] In consequence, wheat stalk (WS), a very plentiful natural nontoxic and biodegradable polymer, is mainly composed of lignocellulosic fibers and minerals[14] (the dry matter of WS is 95%, crude protein 3.6%, crude fat 1.8%, crude fiber 41.2%, nitrogen-free extract 40.9% and ash 7.5%). Moreover, straw is rich in nitrogen, phosphorus, potassium, calcium, magnesium and organic matter.[15] At present, WS is mostly used for returning to the field. However, WS as fertilizer still cannot show its excellent characteristics, and the economic value of this treatment is low. Herein WS, a cost-effective agricultural waste, was rationally selected as a substrate to prepared advanced biodegradable water-retaining agent through attaching acrylic acid (AA) and acrylamide (AAM) onto the WS surface. The core of such design lies in that PAA and PAAM could enhance water absorption. Moreover, the WS substrate has superior adsorption behavior for water due to the hydrophilic state and three-dimensional skeleton. The polymerization of PAA and PAAM supplied a fantastic way to endow the WS with good water absorption, high load capacity and fertilizer manager. On the whole, we can further devise other pre-eminent agricultural waste water retaining agents based on the water holding performance of PAA and PAAM and agricultural waste.

2 Experimental sections

2.1 Materials

Wheat stalk was obtained from a local farm (Shaanxi, China). Acrylamide (AM), acrylic acid (AA), *N*,*N*′-methylenebisacrylamide (MBA), sodium persulfate ($Na_2S_2O_8$), NaOH, and ethanol were supplied by Macklin (Shanghai, China). The above-mentioned materials were used directly without purification.

2.2 Pretreatment of WS

The raw WS was washed ultrasonically in ethanol and deionized water. Then, the WS powders were treated with NaOH solution (2 wt%) under stirring for 1.0 h to remove the adhering substances (wax, *et al.*). Finally, the obtained WS was washed with ethanol and deionized water and dried at 25 °C for 2 days.[11]

2.3 Preparation of WS/PAA–PAM by polymerization

The preparing procedure of WS/PAA–PAM involve of following three steps. First, WS powder was introduced into a 250 mL three-necked flask containing a specified volume of deionized water. The flask was then heated to 55 °C under a nitrogen atmosphere to protect the specimen. The certain amounts of the pretreated AA, AM, and MBA were successively added in a three-necked flask under stirring. The polymerization modification was maintained for 4.0 h. Ultimately, the resulting materials was immersed in ethanol for several times to remove the residual chemicals. Also, the materials without WS were prepared by the above procedures.

2.4 Characterization of WS, PAA–PAM and WS/PAA–PAM

WS, PAA–PAM and WS/PAA–PAM were ground to 60-mesh powder for subsequent characterization. Afterwards, the Fourier transform infrared (FTIR) spectra of the as-obtained samples were recorded in KBr using a PerkinElmer FTIR spectrometer, covering the range of 4000–500 cm^{-1}. The microstructures of WS, PAA–PAM and WS/PAA–PAM were tested by scanning electron microscope (SEM) (Hitachi S-4800).

2.5 Measurements of equilibrium adsorption

To evaluate the water adsorption capacity of the WS and WS/PAA–PAM, the water absorbency of WS and WS/PAA–PAM was tested by a weighing method (*i.e.*, tea bag method). The water is deionized water, and the salt solution is 0.9% NaCl solution. The water absorbency was tested using the procedure described above and calculated using the following formula:

$$Q = (M_t - M_i)/M_i \quad (1)$$

where Q (g g^{-1}) is the water absorbency defined as grams of water per gram of dried specimens and M_t (g) and M_i (g) are the weights of specimens before and after water adsorption, respectively. The equilibrium adsorption amount represents the maximum adsorption capacity of WS and WS/PAA–PAM, beyond which no further increase in adsorption occurs over time.

The re-swelling performance was investigated by the following steps: the 1 g sample was put into a beaker containing 100 mL deionized water for 24 h to ensure complete swelling. Then, the swelling sample was placed at 40 °C for 40 h to dehydrate and record the water holding capacity for a certain interval.

2.6 Slow-release experiments

The slow-release experiments in soils were employed to evaluate the slow-release behavior. For WS, PAA–PAM, and WS/PAA–PAM, 1 g sample was putted into a non-woven bag and buried in dry soil at ambient temperature (25 °C). The soil was kept moist by sprinkling 10 g water one times a day[16] (humidity of 30%). After every day, the materials were dried, and the contents of N and P in the specimens were tested by the Kjeldahl method of distillation and ultraviolet spectrophotometry, respectively.[17] The sustained-release rate could be obtained according to eqn (2):

$$\text{Release rate}(\%) = \frac{m_0 - m}{m_0} \times 100\% \quad (2)$$

Table 1 Primary physico-chemical properties of soil[a]

Soil organic matter (g kg^{-1})	Total nitrogen (g kg^{-1})	Available phosphorus (mg kg^{-1})	Available potassium (mg kg^{-1})	Bulk density (g cm^{-3})	Soil moisture (%)	Sand (%)	Silt (%)	Clay (%)
6.14 ± 0.38 a	1.79 ± 0.09 b	29.77 ± 5.30 a	74.60 ± 19.17 a	1.50 ± 0.52 a	4.84 ± 0.40 ab	44.12 ± 7.59 b	46.60 ± 4.29 a	9.28 ± 1.25 a

[a] Mean ± standard deviation, different lowercase letters in the same column indicate a significant difference at 5% level between treatments.

where m_0 and m are the weights of N (or P) before and after accumulate release.

2.7 Degradation in soil

The soft rock and sand used in this study were collected from Daji Han Village, Xiaoji Han township, Yuyang district, Yulin city. The basic physical and chemical properties of the 0–30 cm soil layer were shown in Table 1.

Flowerpot with about capacity of 5 L were filled with soil. The WS, PAA–PAM, and WS/PAA–PAM were buried in the soil at a depth of 10 cm, respectively. A certain amount of water was added to keep the humidity of the soil. The degree of degradation of the samples was tested at a regular time interval by taking the materials from the soil and cleaning them with distilled water to remove the soil. The specimens were dried in an oven at 40 °C until the weight was constant. Weight loss of the samples with time was conducted to exhibit the degree of degradation in the soil burial process. The soil burial degradation test started on November 10, 2021 and ended on May 10, 2022. The soil burial degradation rate was obtained from the following formula:

$$\text{Degradation rate}(\%) = \frac{W_0 - W_b}{W_0} \times 100\% \quad (3)$$

where W_0 (g) and W_b (g) are the dry weight of the materials before and after soil burial degradation, respectively.

3 Results and discussion

3.1 Formation of WS/PAA–PAM

WS/PAA–PAM was synthesized through the following steps: pretreatment with NaOH solution to expose additional hydroxyl (–OH) groups and remove inherent surface contaminants, followed by aqueous polymerization of PAA–PAM onto the WS surface. The proposed synthesis process and reaction mechanism are illustrated in Scheme 1.

In step 1, WS was dip-treated with NaOH solution to remove the vegetable wax, thereby exposing the reactive –OH groups of lignin and cellulose for subsequent polymerization. The surface of WS is naturally covered with plant wax, which inhibits the polymerization process. Step 2 involves hydrophilic modification, which simultaneously enhances the swelling properties of the substrate. In this step, the hydroxyl groups on WS lose their hydrogen atoms, forming alkoxy radicals in the presence of $Na_2S_2O_8$ initiator. Concurrently, the C=C bonds of acrylate (AC) and acrylamide (AM) break, initiating the polymerization and forming long polymer chains. The alkoxy radicals of WS then

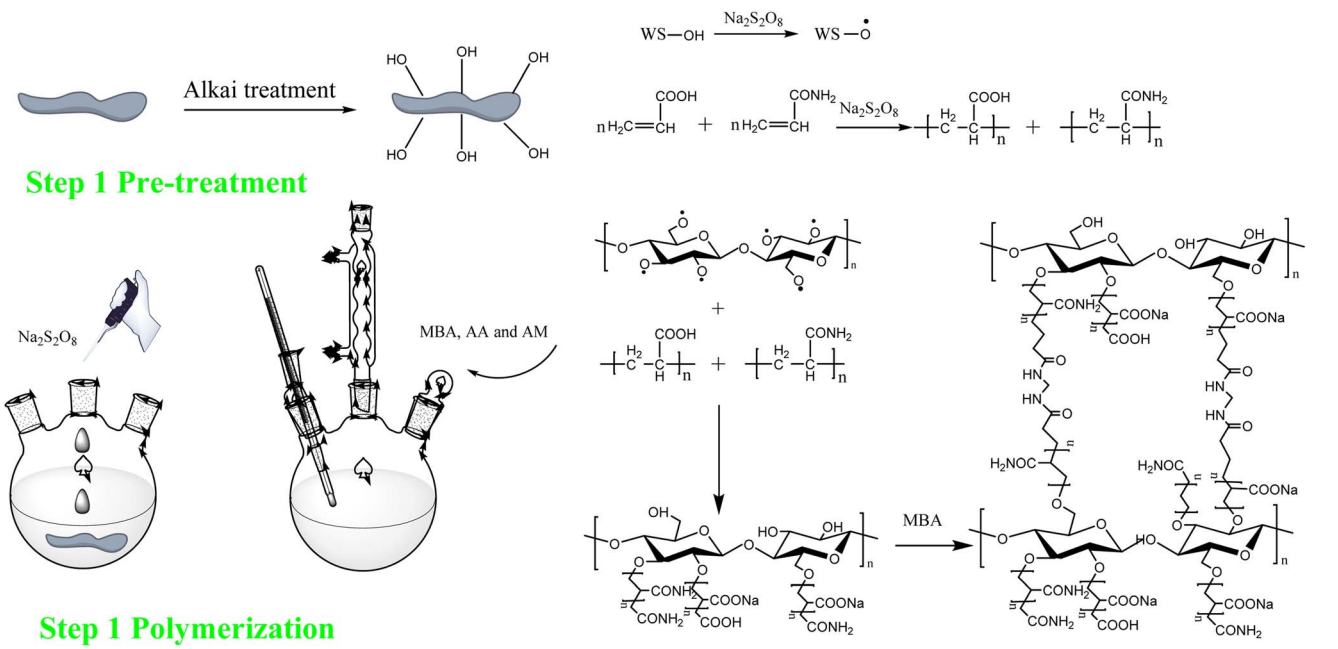

Scheme 1 Proposed formation mechanism of the WS/PAA–PAM.

react with the broken C=C bonds of AC and AM, resulting in the grafting of AC and AM onto the WS matrix.

Based on the composition and structure of WS/PAA–PAM, this material is a promising candidate for use as a water-retaining agent in agricultural applications. First, the WS substrate exhibits superior water adsorption capacity due to its hydrophilic nature and porous structure, which facilitate water absorption.[18] Additionally, as a natural polymer waste, WS is environmentally benign and does not negatively affect soil or crops when used as a water-retaining agent carrier. Moreover, due to its composition, widespread availability, and biodegradability, WS can also be employed as a biofertilizer to supply carbon to soil and crops. Furthermore, the hydrophilic behavior of the WS surface, combined with the low surface energy of PAA–PAM, imparts excellent water-adsorption capacity to WS/PAA–PAM. The network structure of WS enhances its ability to retain water and water-soluble fertilizers, making it suitable as a carrier for sustained release applications.

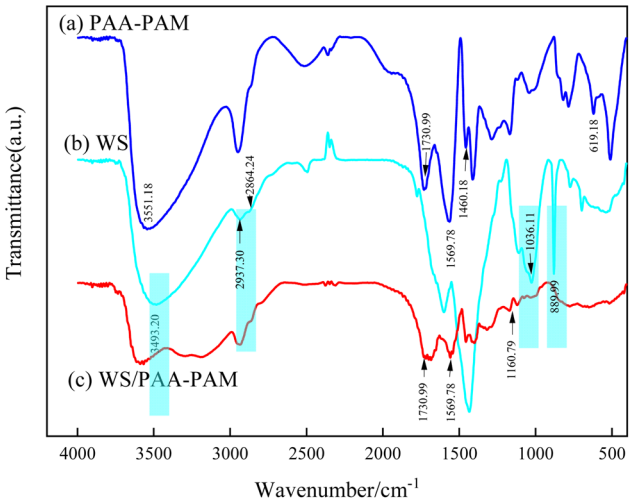

Fig. 2 FTIR spectrometry analysis of PAA–PAM (a), WS (b), WS/PAA–PAM (c).

3.2 Morphology analysis

The surface morphology of specimens was further filed in SEM images. Fig. 1 presents the surface morphology of the WS (a), WS after pretreatment (b), WS/PAA–PAM (c) and (d).

The surface microstructure is closely related to its water absorption properties. Fig. 1 shows the morphology of WS before and after treatment, as well as WS/PAA–PAM and PAA–PAM. As shown in Fig. 1a, the WS is relatively dense and ordered in texture, and the surface of WS is partially covered by a cuticle layer, which leads to a lower accessibility. After alkali treatment (Fig. 1b), the cuticle layer is removed, crystallinity decreases, and the surface becomes rough with many well-defined, ordered voids and pits. The WS/PAA–PAM composite (Fig. 1c) show that the surface structure of the composite material is loose and rough, exhibiting numerous pores. These pores provide ample space for water molecules to infiltrate into the polymer, increasing the contact area between the hydrophilic groups on the polymer chains and the water molecules. This stable network structure facilitates the composite material's ability to absorb a large amount of water.

The surface composition of the as-obtained samples was characterized by FTIR to validate the chemical composition of WS, PAA–PAM, and WS/PAA–PAM. In Fig. 2a, the broad

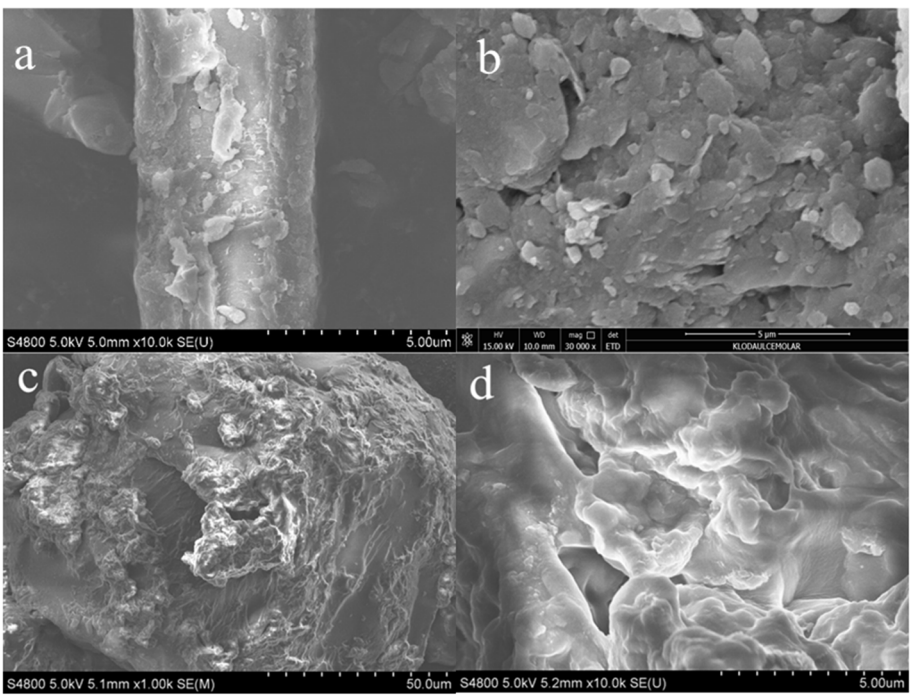

Fig. 1 Comparison of SEM micrographs of WS (a), pre-WS (b), WS/PAA–PAM (c), and PAA–PAM (d).

peaks at 3300–3550 cm^{-1} were ascribed to the stretching vibration of –OH of acrylic acid and $–NH_2$ group of acrylamide. Moreover, adsorption peaks appearing at 1730.99 and1569.78 cm^{-1}, demonstrating the –C=O stretching vibration of acetyl.[19,20] This indicates the formation of AA–AM copolymer. As shown in Fig. 2b, the stretching vibration peak of –OH appears at 3493.20 cm^{-1}. What is more, the characteristic peaks at 1036.11 and 890.00 cm^{-1} were ascribed to the β-1 and 1,4-glycoside bond. The characteristic peaks at 2937.30 and 2864.24 cm^{-1}, attributed to $–CH_2$ stretching vibration.[21] These characteristic peaks are consistent with the infrared spectrum of WS. Additionally, compared with the aforementioned spectra, the WS/PAA–PAM exhibited strong adsorption peak appeared at 1160.79 cm^{-1} due to the interaction between groups of AA, AM WS, which demonstrate the formation of –O– and graft copolymerization product.[22] On the whole, it can be concluded that WS/PAA–PAM had been successfully synthesized.

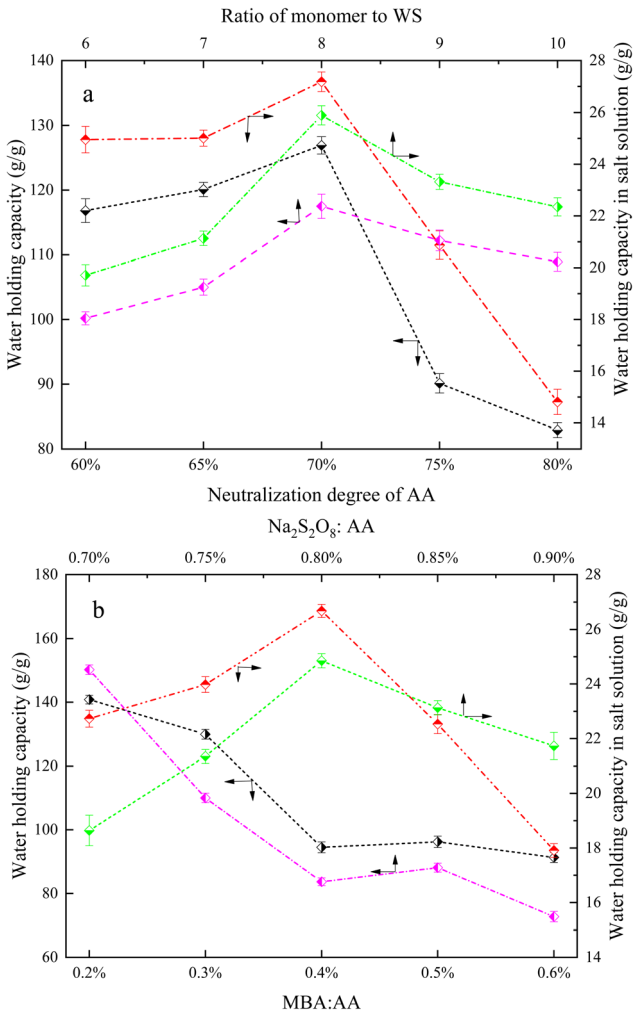

Fig. 3 The different water holding capacity with the degree of neutralization of AA and the ratio of AA and AM to WS (a). Influences of MBA : AA and $Na_2S_2O_8$: AA on the water holding capacity of WS/PAA–PAM (b).

3.3 Water holding capacity of WS/PAA–PAM

Drought restricts water availability for crops, thereby hindering agricultural development.[16,23,24] Water holding capacity of water-retaining agent is the important indicators of agriculture water management. Therefore, to verify the water holding capacity of the material, the comprehensive investigations of water holding capacity of the WS/PAA–PAM, including degree of neutralization of acrylic acid, mass ratio of monomers to WS, are illustrated in Fig. 3.

From Fig. 3a, the water holding capacity firstly increases and then decreases with the increase of the mass ratio of monomer to WS. This phenomenon is due to the increase of AA and AM will lead to the growth of polymerization chain on the surface of WS, thus the hydrophilic group is increased and enhanced the water holding capacity of WS/PAA–PAM.[25] As the amount of AA and AM increased further, the homopolymerization of the excess PAA–PAM could undoubtedly take place, enhancing the steric hindrance and consequently reducing water absorbency. As can also be known from Fig. 3a, the optimum ratio of monomer to WS is 8 : 1. Further, Fig. 3a showed the influence of AA neutralization degree on water holding capacity. At low neutralization degrees, the reaction was difficult to control due to the rapid onset caused by low pH, resulting in products with high crosslinking density and reduced water holding capacity. The maximum water holding capacity occurs when the degree of neutralization is 70%. Nevertheless, the higher neutralization degree would limit the water holding capacity. The additional Na^+ would react with –COO– to form –COONa, thereby reducing electrostatic repulsion, which hindered the expansion of the PAA–PAM network and restricts the space available for water molecules to enter.[26]

The relationships between the water adsorption of WS/PAA–PAM and different amounts of initiator and crosslinking agent were investigated in Fig. 3b. Fig. 3b exhibits the plots of water holding capacity with respect to MBA/AA, showing a downward trend with increasing MBA. This phenomenon can be attributed to the excess cross-linker, which increases network density and shortens chain length, thereby restricting water movement within the WS/PAA–PAM network.[27] A small amount of MBA resulted in a low crosslinking degree, chain length and cross-linking points, which enable the WS/PAA–PAM network structure much looser and large-scale expansion. Hence, more water can enter the network structure. Nevertheless, the small amount of MBA also corresponded to a low structural strength of WS/PAA–PAM. These properties indicate that the suitable dosage of MBA is vital to the structure strength of WS/PAA–PAM and practical application. As can also be infered from Fig. 3b, the optimum ratio of MBA to AA is 0.2%.

From Fig. 3b, it also can be known that the water holding capacity of WS/PAA–PAM was increased greatly as the enhance of initiator reached a maximum at 0.7 wt% and then reduced. As depicted that the role of initiator is to generate primary radicals and initiate WS grafting polymerization with AA and AM. When the amount of $Na_2S_2O_8$ initiator was small, the radicals cannot generate enough active sites in the formation of PAA–PAM chain and make the cross-linked network structure of

WS/PAA–PAM loose. Contrariwise, as more $Na_2S_2O_8$ was used in the polymerization, the chain length of PAA and PAM was shortened due to more free radicals were formed. Meanwhile, as the free radical density increased, the likelihood of effective aggregation and the elastic recoil energy of the crosslinked network also improved. This negatively impacted the WS/PAA–PAM network structure, resulting in reduced water holding capacity. The water holding capacity of WS/PAA–PAM in salt solution is lower than in deionized water, indicating its sensitivity to salt solutions. This phenomenon is attributed to the charge shielding effect of Na^+ in the salt solution, which diminishes electrostatic repulsion and reduces the osmotic pressure between the network and the surrounding medium, leading to a significant decrease in the water adsorption rate.

3.4 Kinetic study

To investigate the water adsorption capacity of the samples, the experimental data were further fitted by using the pseudo-first-order, pseudo-second-order and Ritger–Peppas models as exhibited by the following equation.[28,29]

First order model:

$$\ln(Q_e - Q_t) = k_1 t + L \quad (4)$$

Second order model:

$$\frac{t}{Q_e} = \frac{1}{k_2 Q_e^2} + \frac{t}{Q_e} \quad (5)$$

Ritger–Peppas

$$\frac{Q_t}{Q_e} = k_2 t^n \quad (6)$$

where Q_e and Q_t represent the equilibrium water holding capacity (g g^{-1}) and instantaneous adsorption at any time, respectively. k_1, k_2 and k_3 are the rate constants, t represents the adsorption time (h), L is the intercept, n is the adsorption exponent of adsorption mechanism.[30]

As can be seen in Table 2, the swelling adsorption of WS/PAA–PAM is simulated by using the diffusion model, and the swelling adsorption kinetic parameters of different liquid were calculated to elucidate the swelling process of the WS/PAA–PAM. In Ritger–Peppas formula, n is the characteristic index of the swelling mechanism of WS/PAA–PAM. When n is less than 0.5, the water penetration behavior of WS/PAA–PAM belongs to the Case I diffusion behavior (Fickian diffusion).[31] In this mode, it is mainly the diffusion of water molecules. Clearly, the correlation coefficient of the pseudo-second-order is greater than the pseudo-first-order model and Fickian state of Ritger–Peppas. This phenomenon is due to the pseudo-first-order model is suitable for explaining the single sorption state (physical adsorption or chemical adsorption).[32] Nevertheless, the adsorption of WS/PAA–PAM was controlled by multiple factors (physical adsorption and chemical adsorption). Hence, the pseudo-second-order model is suitable for explaining the water adsorption process of WS/PAA–PAM.

Table 2 Kinetic adsorption parameters of WS/PAA–PAM for deionized water and NaCl solution

Kinetic type	Kinetic constant	Deionized water	NaCl solution
Fick	n	0.45	0.23
	k	0.30	0.53
	R^2	0.9715	0.9800
Pseudo-second-order	k	5.87	4.01
	R^2	0.9987	0.9963
Pseudo-first-order	k	0.242	0.253
	R^2	0.9882	0.9766

3.5 Reusability and water holding capacity

In general, the reusability of WS/PAA–PAM is significant features in the agriculture application. Fig. 4 presents the reusability of the resultant WS/PAA–PAM for reswelling and water holding ability evaluation. Obviously, the maximum water holding capacity of WS/PAA–PAM is downward with the increase of the adsorption cycles, the maximum water holding capacity of second adsorption cycles of WS/PAA–PAM was reduced by 14.81%. For NaCl solution, the maximum water holding capacity of second adsorption cycles was reduced by 9.61%. This phenomenon is due to the repeated process of swelling and drying reduces the crosslinking density of the network structure of WS/PAA–PAM. The release of water from WS/PAA–PAM generally involves two processes. First, the free water contained in the microporous of WS/PAA–PAM was lost, which were assigned to the weak interaction between water molecules and WS/PAA–PAM chains. Then, with the decrease of free water, the water molecules bound to the weaker part of the WS/PAA–PAM molecular chain will also be lost. Finally, the water holding capacity of the WS/PAA–PAM in equilibrium.

3.6 Degradability evaluation of WS/PAA–PAM

A soil burial test has been used to simulate the biodegradability of material in a real soil environment.[33,34] Given that the water retention agent was composed by biodegradable WS, PAA and

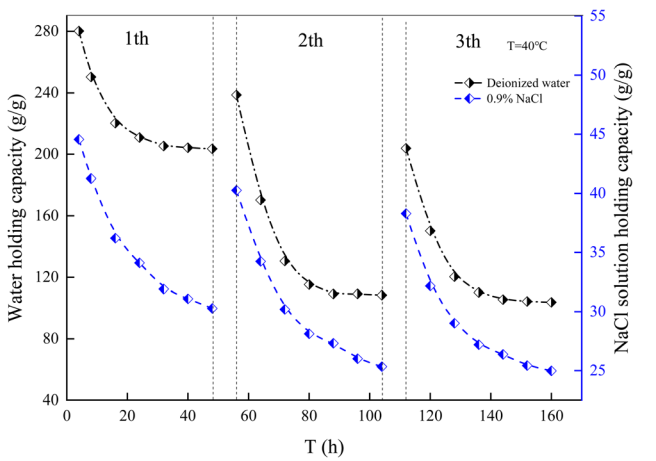

Fig. 4 Reswelling and water holding ability of WS/PAA–PAM.

PAM, the WS/PAA–PAM could be biodegraded in soil. The degradation process of as-obtained materials in soil were evaluated through the soil burial test.

Fig. 5 depicts the degree of soil burial biodegradation plots of the WS, PAA–PAM, WS/PAA–PAM investigated by the weight loss with time. In the first 10 days, a slow degradation behavior occurred initially in WS, PAA–PAM, and WS/PAA–PAM, The phenomenon of short lag phase in Fig. 5 was assigned to the WS, PAA and PAM could be used as carbon and nitrogen source for various microorganisms.[26] Namely, the period of the microorganisms to acclimate to the test samples can be defined lag phase.[26] Further, with the destruction of the microstructure of WS, PAA and PAM by microorganisms, the samples became more readily degradable. During the rapid biodegradation period, the breakdown of the WS, PAA and PAM was accelerated by microorganisms after reproduction. Further, the soil burial degradation process reduced the crosslinking density of the PAA–PAM framework, thereby reducing the swelling rate and the degree of soil burial degradation. Most significantly, the polarity of PAA and PAM allows the mixture to enhance the hydrolysis rate by atmospheric moisture, thereby resulting in the rapid degradation of WS. Then, PAA and PAM could be eventually converted to organic matter and NH_4^+–N by bacterial from soil, respectively.[35,36] Ultimately, the decay of 66.87, 59.2, and 5.6 wt% weight loss was presented, respectively, for the WS, PAA–PAM, WS/PAA–PAM after 120 days of being degraded in soil.

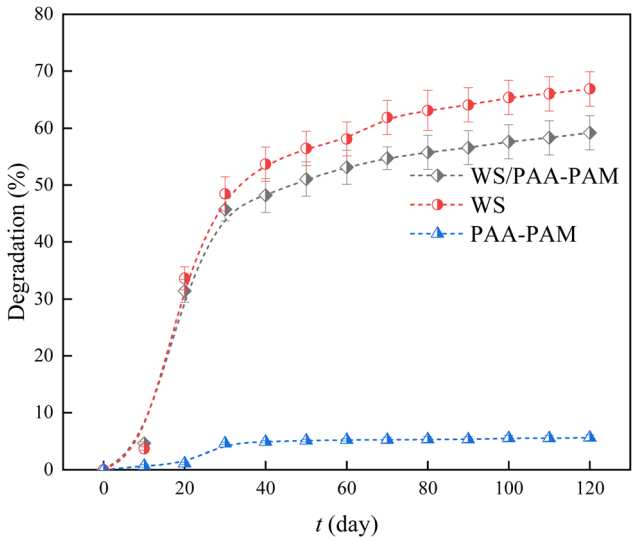

Fig. 5 The degradation of WS, PAA–PAM and WS/PAA–PAM in soil.

Fertilizer, as essential nutrients for plant growth, is a crucial for improve soil fertility and agricultural production.[37,38] It is apparent that the water-soluble fertilizer will be rapidly exhausted through leaching from soil to the groundwater and leads to the reduction of fertilizer utilization and freshwater eutrophication.[39] Although the high fertilizer concentration of the soil can reduce fertilizer rapid loss, the leakage of fertilizer is often risky to environment and ecology.[40,41] In view of the fertilizer utilization, the application of the WS/PAA–PAM with the good water holding capacity might be a feasible fertilizer manager to delay nutrient release to the soil and groundwater. Consequently, urea was employed as a water-soluble fertilizer to evaluate the influence of the diffusion behavior of water and fertilizer on sustained-release behaviors. The results are shown in Scheme 2 and Fig. 6a. The water-retaining agent, composed of WS, AA, and AM, was prepared as described in Scheme 2. After the preparation of the water-retaining agent, the material is capable of loading water and fertilizers such as urea. Due to the interactions of hydrogen bonds, van der Waals forces, and other mechanisms, water and fertilizers are gradually released, providing sustained hydration and nutrition to the soil. During the slow release of water and fertilizers, WS undergoes gradual

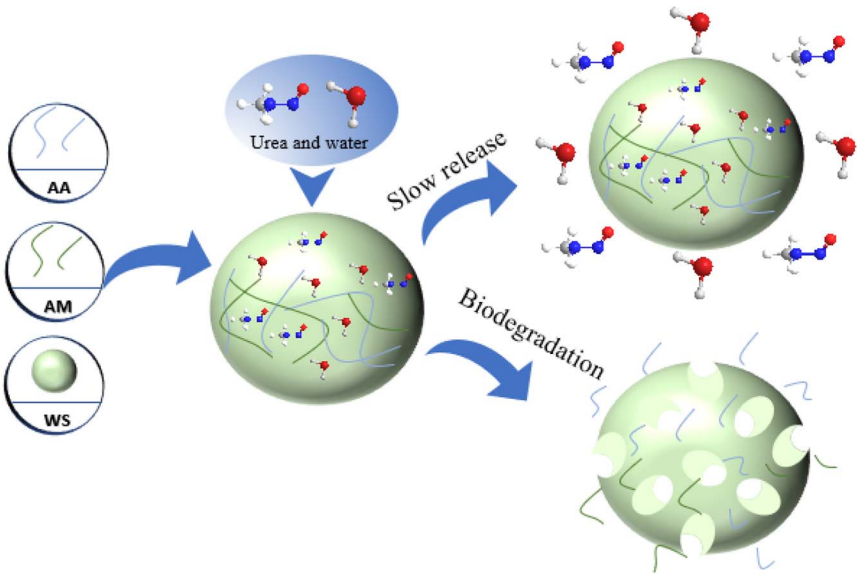

Scheme 2 The release and biodegradation mechanism of the WS/PAA–PAM.

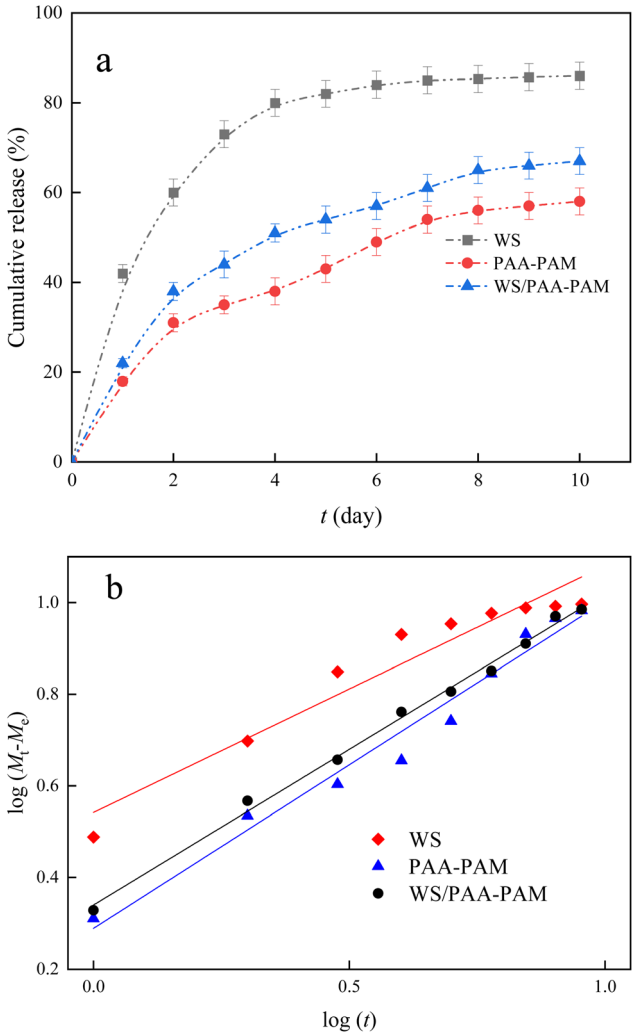

Fig. 6 Cumulative release behaviors of urea from WS, PAA–PAM and WS/PAA–PAM (a). Release kinetics of WS, PAA–PAM and WS/PAA–PAM (b).

degradation under the combined effects of moisture, temperature, and fungi, ultimately breaking down completely in the soil.

From Fig. 6a, the cumulative release rate was about 86.1%, 58.3%, 67.7%, respectively, for the WS, PAA–PAM and WS/PAA–PAM. The results were in agreement with that of water holding capacity, stating clearly that a higher water holding capacity brought about a lower water release ratio and thus a lower urea cumulative release rate in the same time. The PAA–PAM possessed obviously lower fertilizer cumulative release rate than WS and WS/PAA–PAM. This result was owing to the notable characteristics of the denser cross-linked structure and excellent water holding capacity of PAA–PAM designed by polymerization. However, the PAA–PAM is not suitable for water and fertilizer management due to the PAA–PAM degrades slowly and costs more. Compared with PAA–PAM, WS/PAA–PAM is more suitable for agriculture filed, which assigned to the sustained release behaviors and economic performance. In consequence, the sustained release behaviors programmed by polymerization

Table 3 The control release coefficients calculated with the two models

Materials	k	n	R^2	Release mechanism
WS	3.48	0.5387	0.9249	Non-Fickian
PAA–PAM	1.94	0.7141	0.9694	Non-Fickian
WS/PAA–PAM	2.19	0.6795	0.9951	Non-Fickian

method was profit from retaining water-soluble fertilizer in the WS/PAA–PAM, preventing nutrient runoff loss and improving the utilization efficiency of fertilizer.

The sustained-release kinetic data were fitted into the Ritger–Peppas model. The kinetic data are filed in Table 3, and the plots are presents in Fig. 6b. The calculated correlation coefficients (R^2) demonstrate the sustained release of urea from WS/PAA–PAM could be better evaluated by the Ritger–Peppas formula. For WS/PAA–PAM, $0.43 < n < 0.85$, an evidence of both diffusion and swelling controlled urea release (anomalous transport).[42] In consequence, we can conclude from the results in Table 3 and Fig. 4b that the sustained release of urea from WS/PAA–PAM was controlled through free diffusion of concentration gradient and the swelling behavior of the network of WS/PAA–PAM by the relaxation of macromolecular chains of PAA–PAM.

3.7 Practical application

To evaluate the water retention capacity in the soil system, the RH of soil with and without the use of water retaining agents were recorded. From Fig. 7, the humidity fluctuates greatly in pure soil environment. Compared to the pure soil systems, the soil system moisture decreases slowly after using water retaining agents. Similarly, we recorded the RH of different potted plants at 4 p.m. for 10 consecutive days. The results showed that the RH with WS/PAA–PAM was about 61% compared to about 33% for the soil-only system. These results showed that the WS/

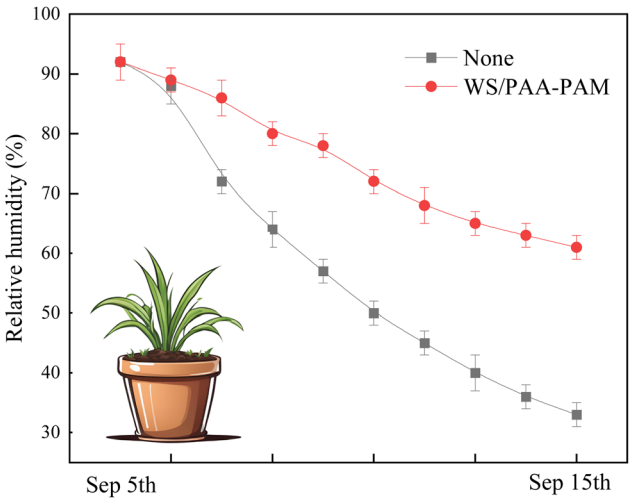

Fig. 7 The RH of soil with and without the use of water retaining agents.

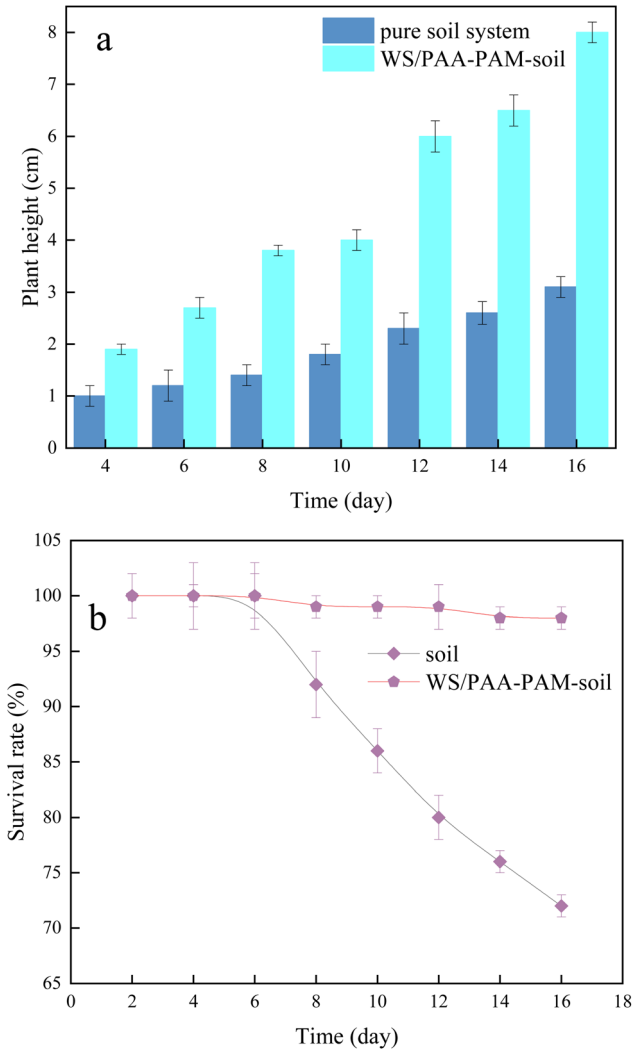

Fig. 8 (a) Plant height with the WS/PAA–PAM-soil and the soil-only systems in 16 days. (b) Survival rate of *Lolium perenne* L. in the WS/PAA–PAM-soil and the soil-only systems in 16 days.

PAA–PAM possess the ability to reduce soil moisture loss. The high-water content favors agricultural cultivation.

To compare the effects of using water retention agents on plant growth, the pot experiments were conducted to verify its practical use. Under relatively stable relative humidity conditions of WS/PAA–PAM-soil, *Lolium perenne* L. can grow to 7.6 cm in 16 days. Nevertheless, the *Lolium perenne* L. height can only reach to 3.1 cm in the pure soil system (Fig. 8a). Furthermore, the survival rates of *Lolium perenne* L. in both WS/PAA–PAM-soil and soil-only systems, further validate the feasibility of our WS/PAA–PAM-soil-based sustainable agricultural system. In the WS/PAA–PAM-soil system, the survival rate of *Lolium perenne* L. remained at 98% after 16 days, while the control group in the soil-only system showed a 72% survival rate after just 14 days (Fig. 8b). These results suggest that the incorporation of WS/PAA–PAM into the soil significantly enhances water retention and supports plant growth under conditions of limited water availability. The improved survival rate and height of *Lolium perenne* L. in the WS/PAA–PAM-soil system highlight the potential of this system for sustainable agricultural practices, especially in regions where water scarcity is a concern. Moreover, the effectiveness of the WS/PAA–PAM-soil system over traditional soil-based systems underscores the potential for its widespread application in enhancing crop resilience and reducing water consumption in agricultural settings.

4 Conclusion

In conclusion, this work proposed a simple approach for the biodegradable WS/PAA–PAM water holding material using a straightforward polymerization method. Notably, the enhanced hydrophilic polymer was decorated onto the surface through polymerization with AA and AM. In terms of structure and composition, the resultant WS/PAA–PAM demonstrated superior performances in water holding capacity and reusability. Specifically, WS/PAA–PAM exhibited a maximum water absorption capacity of 273.54 g g^{-1} in deionized water and 44.54 g g^{-1} in a 0.9% NaCl solution. Furthermore, after three cycles of swelling, the material retained a high water absorption capacity of over 200 g g^{-1}. After being placed in a 40 °C environment for 48 hours, it maintained a water holding capacity of 100 g g^{-1}. Additionally, as a simple method to construct a loaded fertilizer carrier, the hydrophilic state and adsorption performance may promote immediate applications in fertilizer management areas. Moreover, WS/PAA–PAM presented excellent biodegradability, further enhancing its potential in agricultural applications. Benefiting from its superior water holding performance, we consider WS/PAA–PAM to be a promising candidate to replace conventional water-retaining agents in soil, effectively addressing agricultural water shortages and frequent irrigation issues. We also believe that this biodegradable water-retaining agent and water-soluble fertilizer carrier will inspire the development of other water holding materials utilizing agricultural waste.

Data availability

The datasets generated and/or analysed during the current study are available in the science data bank repository, **https://www.scidb.cn/en/anonymous/QUpKWkJ2**.

Conflicts of interest

The authors declare that they have no known competing financial interests or personal relationships that could have appeared to influence the work reported in this paper.

Acknowledgements

This work was also supported by the key research and development program of Shaanxi (Program No. 2023-ZDLNY-48, 2024NC-YBXM-245), Shaanxi Provincial Land Engineering Construction Group internal research project (DJNY2024-31, DJNY2024-08).

References

1 J.-J. Dethier and A. Effenberger, *Econ. Syst.*, 2012, **36**, 175–205.
2 R. T. Arnold, C. Troost and T. Berger, *Water Resour. Res.*, 2015, **51**, 648–668.
3 Z. Qi and X. Hu, *Eur. Polym. J.*, 2022, **166**, 111045.
4 M. Tanveer, A. Farooq, S. Ata, I. Bibi, M. Sultan, M. Iqbal, S. Jabeen, N. Gull, A. Islam, R. U. Khan and S. H. Al-Mijalli, *Surf. Interfaces*, 2021, **25**, 101285.
5 C. Liu, F. Lei, P. Li, J. Jiang and K. Wang, *Carbohydr. Polym.*, 2020, **236**, 116100.
6 W. Wang, S. Yang, A. Zhang and Z. Yang, *Sci. Total Environ.*, 2021, **768**, 144978.
7 L. Chang, L. Xu, Y. Liu and D. Qiu, *Polym. Test.*, 2021, **94**, 107021.
8 Y. Shen, H. Wang, Z. Liu, W. Li, Y. Liu, J. Li, H. Wei and H. Han, *J. Ind. Eng. Chem.*, 2021, **93**, 375–382.
9 W. Wang, S. Yang, A. Zhang and Z. Yang, *J. Appl. Polym. Sci.*, 2020, **137**, 48951.
10 J. Song, L. Li, Y. H. Niu, R. Y. Ke and X. Zhao, *J. Appl. Polym. Sci.*, 2022, 52182.
11 Y. Chenxi, L. Juan, W. Jian, G. Zhen, W. Huanyuan, S. Chendi, H. Dongwen and L. Ling, *New J. Chem.*, 2020, **44**, 15983–15993.
12 A. Sarkar, J. A. Azim, A. A. Asif, L. Qian and A. K. Peau, *Land Use Policy*, 2021, **109**, 105638.
13 M. Khanna, S. M. Swinton and K. D. Messer, *Appl. Econ. Perspect. Pol.*, 2018, **40**, 38–59.
14 S. R. A. Collins, N. Wellner, I. Martinez Bordonado, A. L. Harper, C. N. Miller, I. Bancroft and K. W. Waldron, *Biotechnol. Biofuels*, 2014, **7**, 121.
15 A. R. Barzegar, A. Yousefi and A. Daryashenas, *Plant Soil*, 2002, **247**, 295–301.
16 D. Feng, B. Bai, H. Wang and Y. Suo, *J. Agric. Food Chem.*, 2017, **65**, 5896–5907.
17 M. R. Martins, L. F. Sarkis, S. A. C. Sant'Anna, C. A. Santos, K. E. Araujo, R. C. Santos, E. S. AraÚJo, B. J. R. Alves, C. P. Jantalia, R. M. Boddey, M. Zaman and S. Urquiaga, *Pedosphere*, 2021, **31**, 243–254.
18 L. Liu, S. Zou, H. Li, L. Deng, C. Bai, X. Zhang, S. Wang and N. Li, *Energy Build.*, 2019, **201**, 19–36.
19 F. Dong, J. Wang, Y. Wang and S. Ren, *J. Mater. Chem.*, 2012, **22**, 11093–11100.
20 Q. Lv, M. Wu and Y. Shen, *Colloids Surf. A Physicochem. Eng. Asp.*, 2019, **583**, 123972.
21 L. Shang, J. Ahrenfeldt, J. K. Holm, A. R. Sanadi, S. Barsberg, T. Thomsen, W. Stelte and U. B. Henriksen, *Biomass Bioenergy*, 2012, **40**, 63–70.
22 L. Xie, M. Liu, B. Ni and Y. Wang, *Ind. Eng. Chem. Res.*, 2012, **51**, 3855–3862.
23 G. Bodner, A. Nakhforoosh and H.-P. Kaul, *Agron. Sustain. Dev.*, 2015, **35**, 401–442.
24 V. H. D. Zuazo, I. F. García-Tejero, B. C. Rodríguez, D. F. Tarifa, B. G. Ruiz and P. C. Sacristán, *Agron. Sustain. Dev.*, 2021, **41**, 13.
25 A. I. Abd-Elhamid and A. A. Nayl, *J. Mater. Res. Technol.*, 2021, **15**, 3807–3824.
26 W. Kong, Q. Li, X. Li, Y. Su, Q. Yue and B. Gao, *J. Environ. Manage.*, 2019, **230**, 190–198.
27 J. Hai, B. Bai, C. Ding, H. Wang and Y. Suo, *Polym. Compos.*, 2018, **39**, 1051–1063.
28 B. K. Preetha and B. Vishalakshi, *Int. J. Biol. Macromol.*, 2020, **154**, 739–750.
29 G.-B. Li, J. Wang and X.-P. Kong, *Carbohydr. Polym.*, 2020, **249**, 116865.
30 B. Thakur, G. Sharma, A. Kumar, S. Sharma, M. Naushad, J. Iqbal and F. J. Stadler, *J. Mol. Liq.*, 2020, **319**, 114166.
31 F. E. Koc and T. G. Altıncekic, *Polym. Bull.*, 2021, **78**, 3383–3398.
32 Q. Gao, X. Wang, H. Wang, D. Liang, J. Zhang and J. Li, *Mater. Lett.*, 2019, **254**, 149–153.
33 N. L. Tai, R. Adhikari, R. Shanks and B. Adhikari, *Int. Biodeterior. Biodegrad.*, 2019, **145**, 104793.
34 S. Baidurah, P. Murugan, K. Y. Sen, Y. Furuyama, M. Nonome, K. Sudesh and Y. Ishida, *J. Anal. Appl. Pyrolysis*, 2019, **137**, 146–150.
35 Y. Ma, Y. Sun, Y. Fu, G. Fang, X. Yan and Z. Guo, *Chemosphere*, 2016, **163**, 610–619.
36 A. Nyyssölä and J. Ahlgren, *Int. Biodeterior. Biodegrad.*, 2019, **139**, 24–33.
37 D. Bhardwaj, M. W. Ansari, R. K. Sahoo and N. Tuteja, *Microb. Cell Factories*, 2014, **13**, 66.
38 A. Cai, M. Xu, B. Wang, W. Zhang, G. Liang, E. Hou and Y. Luo, *Soil Tillage Res.*, 2019, **189**, 168–175.
39 C. Weihrauch and C. J. Weber, *Sci. Total Environ.*, 2021, **796**, 149037.
40 A. J. Capellesso, A. A. Cazella, A. L. Schmitt Filho, J. Farley and D. A. Martins, *Agroecol. Sustain. Food Syst.*, 2016, **40**, 215–236.
41 A. O. Numbere, in *Sustainable Intensification for Agroecosystem Services and Management*, ed. M. K. Jhariya, A. Banerjee, R. S. Meena, S. Kumar and A. Raj, Springer Singapore, Singapore, 2021, pp. 615–655, DOI: **10.1007/978-981-16-3207-5_17**.
42 J. Siepmann and N. A. Peppas, *Adv. Drug Delivery Rev.*, 2012, **64**, 163–174.